AFRL-DE-TR-
1999-1026

High-Power Triggered Gas Switches

David V Giri, Vic Carboni, and Ian Smith

Pro-Tech
1630 North Main Street, #377
Walnut Creek, CA 94596-4609

28 June 1999

Final Report

APPROVED FOR PUBLIC RELEASE; DISTRIBUTION IS UNLIMITED.

20000128 033

AIR FORCE RESEARCH LABORATORY
Directed Energy Directorate
3550 Aberdeen Ave SE
AIR FORCE MATERIEL COMMAND
KIRTLAND AIR FORCE BASE, NM 87117-5776

DTIC QUALITY INSPECTED 1

AFRL-DE-TR-1999-1026

Using Government drawings, specifications, or other data included in this document for any purpose other than Government procurement does not in any way obligate the U.S. Government. The fact that the Government formulated or supplied the drawings, specifications, or other data, does not license the holder or any other person or corporation; or convey any rights or permission to manufacture, use, or sell any patented invention that may relate to them.

This report has been reviewed by the Public Affairs Office and is releasable to the National Technical Information Service (NTIS). At NTIS, it will be available to the general public, including foreign nationals.

If you change your address, wish to be removed from this mailing list, or your organization no longer employs the addressee, please notify AFRL/DEHP, 3550 Aberdeen Ave SE, Kirtland AFB, NM 87117-5776.

Do not return copies of this report unless contractual obligations or notice on a specific document requires its return.

This report has been approved for publication.

Dr Jane Lehr, DR-II
Project Manager

FOR THE COMMANDER

MARK FRANZ, Lt Col, USAF
Chief, High Power Microwave Division

R. EARL GOOD, SES
Director, Directed Energy

REPORT DOCUMENTATION PAGE

Form Approved
OMB No. 074-0188

Public reporting burden for this collection of information is estimated to average 1 hour per response, including the time for reviewing instructions, searching existing data sources, gathering and maintaining the data needed, and completing and reviewing this collection of information. Send comments regarding this burden estimate or any other aspect of this collection of information, including suggestions for reducing this burden to Washington Headquarters Services, Directorate for Information Operations and Reports, 1215 Jefferson Davis Highway, Suite 1204, Arlington, VA 22202-4302, and to the Office of Management and Budget, Paperwork Reduction Project (0704-0188), Washington, DC 20503

1. AGENCY USE ONLY (Leave blank)	2. REPORT DATE	3. REPORT TYPE AND DATES COVERED
	28 June 1999	Final Report, 1 May 98 – 28 June 99

4. TITLE AND SUBTITLE
High-Power Triggered Gas Switches

5. FUNDING NUMBERS
C: F29601-98-C-0151
PE: 65502F
PR: 3005
TA: DO
WU:AB

6. AUTHOR(S)
David V Giri, Vic Carboni, Ian Smith

7. PERFORMING ORGANIZATION NAME(S) AND ADDRESS(ES)

Pro-Tech
1630 North Main Street #377
Walnut Creek, CA 94596-4609

8. PERFORMING ORGANIZATION REPORT NUMBER
PT/DFR 99-01

9. SPONSORING / MONITORING AGENCY NAME(S) AND ADDRESS(ES)

Air Force Research Laboratory / Directed Energy
3550 Aberdeen Ave SE
Kirtland AFB, NM 87117-5776

10. SPONSORING / MONITORING AGENCY REPORT NUMBER
AFRL-DE-TR-1999-1026

11. SUPPLEMENTARY NOTES
This report is prepared on cooperation with TITAN Pulse Sciences, Inc., 600 McCormick Street, San Leandro, CA 94577

12a. DISTRIBUTION / AVAILABILITY STATEMENT
Approved for Public Release; Distribution is Unlimited.

12b. DISTRIBUTION CODE

13. ABSTRACT *(Maximum 200 Words)*

Examples of ultrawide band sources using self-closing spark-gap type of gas switches are the H-series systems at Air Force Research Laboratory. There are several reasons to build triggered versions of the basic high-voltage spark gap. They include synchronization with an external event, timed-array antenna for steering directed energy systems etc. Phase I includes a systematic formulization of a short pulse testbed facility. The fabrication and delivery of the facility is proposed for a Phase II effort. The designed facility is modular and capable of studying different types of electrical and laser triggering, gas mixes, electrode geometries, etc. The conceptual layouts and electrical field calculations have been completed in the critical stressed regions of the system. The 2-D transmission line code was used to model the circuit and preliminary runs were made. The contractor intends to develop this further in the Phase II effort and predict waveshapes.

14. SUBJECT TERMS
triggered switches, gas switches, laser trigger, UWB sources, jitter, transient arrays

15. NUMBER OF PAGES
46

16. PRICE CODE

17. SECURITY CLASSIFICATION OF REPORT	18. SECURITY CLASSIFICATION OF THIS PAGE	19. SECURITY CLASSIFICATION OF ABSTRACT	20. LIMITATION OF ABSTRACT
UNCLASSIFIED	UNCLASSIFIED	UNCLASSIFIED	UNLIMITED

NSN 7540-01-280-5500

Standard Form 298 (Rev. 2-89)
Prescribed by ANSI Std. Z39-18
298-102

Contents

Section		Page
1.	Introduction	1
2.	Objectives of Phase I Effort	4
3.	The Overall Pulser / Radiating System	6
4.	The Pulser as a Testbed System	9
	4.1 Design Approach	9
	4.2 Utility of this System	16
	4.3 Measurements	21
5.	Description of the Radiating System	22
	5.1 Canonical Input Waveforms to the Radiating System	22
	5.2 Half-Cycle Sine Wave	22
6.	Prediction of Far Fields for a Single Antenna Element	25
7.	Optimization of a Three Element Array	28
8.	Objectives of Phase II Effort	31
	8.1 Introduction to Phase-II	31
	8.2 Phase-II Technical Objectives	33
	References	36

List of figures

Figure		Page
Figure 1.	Block Schematic of the Testbed Pulser and the Radiating Sytem	7
Figure 2.	The Marx and the Testbed Pulser with a Vertical Axis	8
Figure 3.	Simplified Circuit	10
Figure 4.	Overall Configuration : Plan View	12
Figure 5.	Switch Configuration	13
Figure 6.	Gas Breakdown Data	19
Figure 7.	The Half-cycle Sine Wave and its Spectral Magnitude	24
Figure 8.	A spherical TEM horn element and its source point in the aperture plane	26
Figure 9.	Radiated Electric Field from an Individual TEM horn in the two planes for the case of a Half-cycle Sine Wave Input Shown in the Middle	29
Figure 10.	A Generalized Timed-Array Antenna Distribution	30
Figure 11.	Milestone and Schedule for the Proposed Phase-II Effort	32

List of Tables

Table		Page
Table 1.	Design goals.	6
Table 2.	Effective Stress Times for the two Switches	18
Table 3.	Fields that could be achieved with Nitrogen and Hydrogen Gas at 100 atm	20
Table 4.	Expected Risetimes for the two Switches at 100 atm.	21
Table 5.	Technical Performance Goals	34

This page has been intentionally left blank.

1. Introduction

GAs spark gap switches have been used in a number of Ultra Wide Band (UWB) sources, in particular the Hindenberg series built by Air Force Research Laboratory (AFRL) and the prototype Impulse Radiating Antenna (IRA) built ty Pro-Tech and Pulse Sciences, Incorporated (PSI). All these have used high pressure hydrogen; at AFRL in order to achieve > 1kHz prf and in the prototype IRA pulser (PSI) in order to minimize risetime in a voltage range where this is theoretically dominated by resistive phase. Other gases (nitrogen, air, SF6-mixed), can be used advantageously for lower repetition rates.

All the systems mentioned have employed self-closing switches charged in hundreds of nanoseconds to generate the basic high voltage pulse. In some cases additional peaking or sharpening switches have been used to achieve the desired < 200 ps risetime; these are very fast charged and have sub-nanosecond jitter. The overall jitter of the system is dominated by the self-closure of the basic high voltage spark gap, and is typically ~ 10 nsec (1s). The prime power switch used to charge the high voltage spark gas is a triggered switch—usually a thyratron or another hydrogen switch is used to allow >1 kHz prf—and while the jitter of this is typically smaller, in the nanosecond range, this would not be negligible in other applications of interest.

There are a number of motives for developing triggered versions of the basic high voltage spark gap, and there are as follows.

(1) ***Synchronization with another event:*** in some cases the present ~10 ns jitter may be adequate, while in others triggering of the high voltage switch may be needed to eliminate both it's self-closing jitter and also to eliminate the jitter of the primary switch from the system jitter.

(2) ***Eliminating shot-to-shot variation associated with self-closing jitter:*** in interference applications this is unimportant, but for target analysis in radar applications it may be very important. A jitter of ~ 1 ns could be adequate, the exact value depending on the charge time.

(3) ***Switchout at peak pulse charge;*** where the residual circuit energy is minimal. Self-closing switches will normally not close at peak charge, and in fact must usually be set with an average closure time well before peak to ensure that they do close. The residual energy left in the charging circuit has several disadvantages, including: adding to the prime power required; prolonging current flow in the switches, delaying recovery and reducing the maximum prf; and decreasing the life of capacitors and switches by increasing reversal and charge transfer.

(4) ***Synchronization and possibly electronic steering of an array of UWB sources*** [1] **:** This definitely requires triggering of the high voltage switch, and the jitter must be much less than the risetime, thus in the range of a few ps to a few tens of ps.

(5) ***To produce multi-channelling*:** The risetime of many gas switches is limited by their inductance. A switch that self-closes under a ~ 200 nsec charge closes in one channel, which means an inductance ~ 10 nH/cm, or at a 1-1.5 MV/cm field typical of such a switch 7-10 nH/MV. For a typical 100 ohm antenna impedance, the 10-90% inductance risetime will be ~ 2 L/R ~ 150-200 ps per MV. Multi-channel triggering can reduce this in proportion to the number of channels created, as long as the channels do not vary in their transit time from the source aperture by a significant fraction of the risetime.

Another risetime limitation is the resistive phase. This calculates to be 90-150 ps independent of voltage for hydrogen at ~ 100 at., according to J.C. Martin's formula [2]. Multi-channeling also reduces the resistive phase, though according to Martin's formula less than linear with the number of channels, so that depending on the voltage, once a few channels are created the resistive phase will dominate, and increasing the number of channels further will reduce the risetime more slowly. So, it may be difficult to get much below 50-100 ps. Whether this is really correct is uncertain, because Martin's result was derived from data for gases operating at much lower fields than are of interest here; in the case of the prototype IRA, where the relatively low voltage means that the calculated resistive phase should dominate over the inductive contribution, experimental results suggest that the actual resistive phase may be smaller than is given by Martin's formula, as has been observed in oil. In that case, multi-channeling will have a larger effect.

The source risetime can be decreased by using the triggered high voltage switch to fast-charge a peaking or sharpening switch that closes at higher field and thus has reduced inductive and resistive phases, or that multichannels because of the ultra-rapid charging, in either case overcoming the risetime limitations of the first switch. Even in this case, multi-channeling of the first switch can help substantially by speeding charge of the second switch, and perhaps also by allowing the first switch to provide enough current to charge an array of second switches.

1.1 Electrical Triggering

In the "trigatron" a discharge in one electrode causes breakdown by photo-ionization or by injection of arc plasma into the main gap. The design of trigatrons is a compromise between maximizing the perturbation produced by the spark and minimizing the degradation produced by the trigger region;

degradation is especially severe at high gas pressures. Use of a high permittivity dielectric around the trigger pin minimizes the degradation, but inhibits recovery for high prf. The jitter of trigatrons is typically higher than those of the other types, and multi-channel trigatrons have rarely been achieved.

Another possibility is a three electrode trigger switch with a trigger electrode that is pulsed to over-volt the two halves of the switch in turn as uniform field switches. Breakdown is often regularized by UV illumination from an auxiliary trigger spark, as illustrated, though the high fields of interest for UWB switches this is probably made unnecessary by the electrons field-emitted from the cathode. Especially without the auxiliary illuminator, this approach should be compatible with short risetimes and high prf; but it has not been shown capable of multi-channeling.

It is also feasible to provide the trigger electrode with a small radius edge that initially has little field enhancement because it lies on an equipotential, but which when pulsed develops field enhancement in addition to the increased voltages and average fields on the successive gap sides [3]. The critical process is the formation of streamers in the trigger edge region, which depends on the local field and its enhancement, so the trigger region need not increase in proportion to the gap. Trigger voltages of $\sim$ 200 kV and trigger gaps of $\sim$ 0.5 cm readily yield such nanosecond jitter and multi-channels, especially in gases like SF_6 where edges of one particular polarity are very weak. This has been demonstrated at up to 3 MV [4]. For 1 MV gaps, Carboni demonstrated very dense multi-channeling in SF_6 gas mix, [5].

Because the streamer formation distances shorten as the pressure and field rise, high pressure, high field UWB gaps should incorporate the three-electrode trigger technique very readily, provided that the trigger electrode potential can be accurately maintained during charge. For moderate prf's, SF_6 mixes are ideal because of their polarity effect. For higher repetition rates, H_2 will be preferred; its polarity effect may be identifiable from the available literature.

1.2 Laser Triggering

In the most commonly used method of laser triggering, the laser beam is introduced axially through a hole in one electrode and is focussed in the gap. The intensity is sufficient that the laser fields alone break down the gas over some distance near the focus. This produces an axial line spark that rapidly propagates to join the electrodes, under the switch field.

Depending somewhat on the gas, and its density, the laser needs a power density of order 10^{10} W/cm^2 at the focus. The ability to reach this level and the extent of the region over which it exists are easily calculated from the beam power, the divergence, and the optics. For the high pressures used in

UWB switches the power density needed will be large, but the length over which it is needed will be small because of the short critical breakdown distances.

Jitters much less than 1 ns have been demonstrated using the axial laser triggering approach. Previous results at PSI have shown that 100 kV switches with a gap spacing of 1 cm and using SF_6 and air at pressures of up to 50 psig have exhibited rms closure jitter of about 130 ps using as low as 8 mJ of 266 nm light, even when the switch was operated at 50% of self-breakdown voltage. The results have seemed to confirm the necessity of obtaining ~ 10^{10} watts/cm^2 in the gas to produce breakdown. Multi-channeling, however, has not been commonly achieved with this technique. It clearly requires several adjacent laser beams. Workers at Rutherford Appleton Labs have reported achieving 2-3 channels on average out of four triggered sites in an SF_6 switch (Mick Shaw, RAL, private communication).

It is also feasible to have a transverse illumination scheme used in a rail gap at the High Voltage Institute, Gottingen. Channels spaced only a few mm apart were stably generated, using a modest laser power density, at 10 Hz for long periods, (S. Szatmari, private communication and [6]). If this technique can be applied to UWB spark gaps in the form of short rail gaps (or wide rail gaps driving a wide TEM horn) it will clearly be preferred over the axial triggering.

2. Objectives of Phase-I Effort :

The first objective of Phase-I was to investigate the basic feasibility of the various triggering schemes discussed previously to UWB spark gaps. The investigation included review of the literature and discussions with workers in the field to improve understanding of the techniques and how they apply to very dense, high field gases and to hydrogen in particular. The goal was to select the most promising triggering approach from those discussed. The objectives of both Air Force and commercial applications were taken into account, e.g. in deciding what are lower repetition rates of interest and hence what emphasis should be placed on gas in addition to hydrogen. The requirements for the most promising techniques were used to design a test bed. The ultimate objective of Phase-I was to produce a design for a test bed that can be fabricated and used in Phase-II to investigate the feasibility of optically and electrically triggering very fast gas switches and to demonstrate one or more triggered switches for use in UWB sources.

The uniqueness of the test bed design is its flexibility to study the triggerability and jitter of fast switches with various types of gases and mixtures, including H_2 to pressures of 100+

atmospheres, with a variety of electrode configurations and a number of materials, and with both electrical and optical triggering schemes. In addition to its primary use as a test bed, it will also be designed to be easily adaptable to be connected to an actual antenna such as a TEM horn or 1/2 IRA for use as a practical UWB

The objective of Phase-I was to develop the conceptual design for a triggered ultra-wide band (UWB) source spark gap with a jitter on the order of 10's of ps. The ability to do this would enable one to:

- synchronize the spark gap closure with another event;
- eliminate shot-to-shot variation associated with a self-breaking switch;
- switch out closer to full charge voltage to minimize the potentially damaging residual stored energy in a system that is left behind;
- synchronize spark gaps within a UWB array to enable one to steer the beam; and
- produce a multi-channeling primary switch that can result in lower inductance and resistive phase that could ultimately eliminate the need for a secondary peaking switch.

In Phase-I we have focussed on the use of a triggered gas switch employing both electrical triggering and laser triggering methods.

As a secondary objective, the design concept was to couple the triggered switch to a peaking circuit to form a test bed that could be used in the laboratory to produce a fast output pulse. The pulser concept was such that it could be connected to one or three antennas such as TEM horns or half IRAs for use as a practical UWB source.

The ultimate goal was to fabricate and test the hardware in a subsequent Phase-II program.

The design goals for the test bed are given in Table 1

Table 1. Design goals.	
Output voltage	~ 500 kV
Output risetime (10-90%)	~ 100 ps
dV/dt	5×10^{15} V/sec
Pulse length (e-fold)	~ 5 nsec
Rep-rate Self-breaking and electrically triggered Laser (YAG)	 50 Hz ~ 10 Hz
Driven load impedance	~ 67 - 135 ohms
Jitter goal (1 standard deviation rms)	10-20 psec

3. The overall Pulser / Radiating System

The block schematic of the complete system is shown in figure 1. The basic components are: 1) power supplies, 2) controls, 3) gas handling controls, 4) Marx trigger, 5) a 500 kV Marx, 6) a triggered switch, 7) a self-breaking peaking switch, 8) 1:3 splitter, 9) an array of 3 TEM horn antennas.

The details of each of the pulser elements are discussed in the following section. The TEM horn antenna design and fabrication is straightforward. The optimization of the horn geometry is done by analysis and experimental data. However, the key element here is the 1:3 splitter. This element remains to be designed/developed under the Phase-II effort. The Marx and the testbed pulser with a vertical axis is shown in figure 2. This figure does not include the 1:3 splitter.

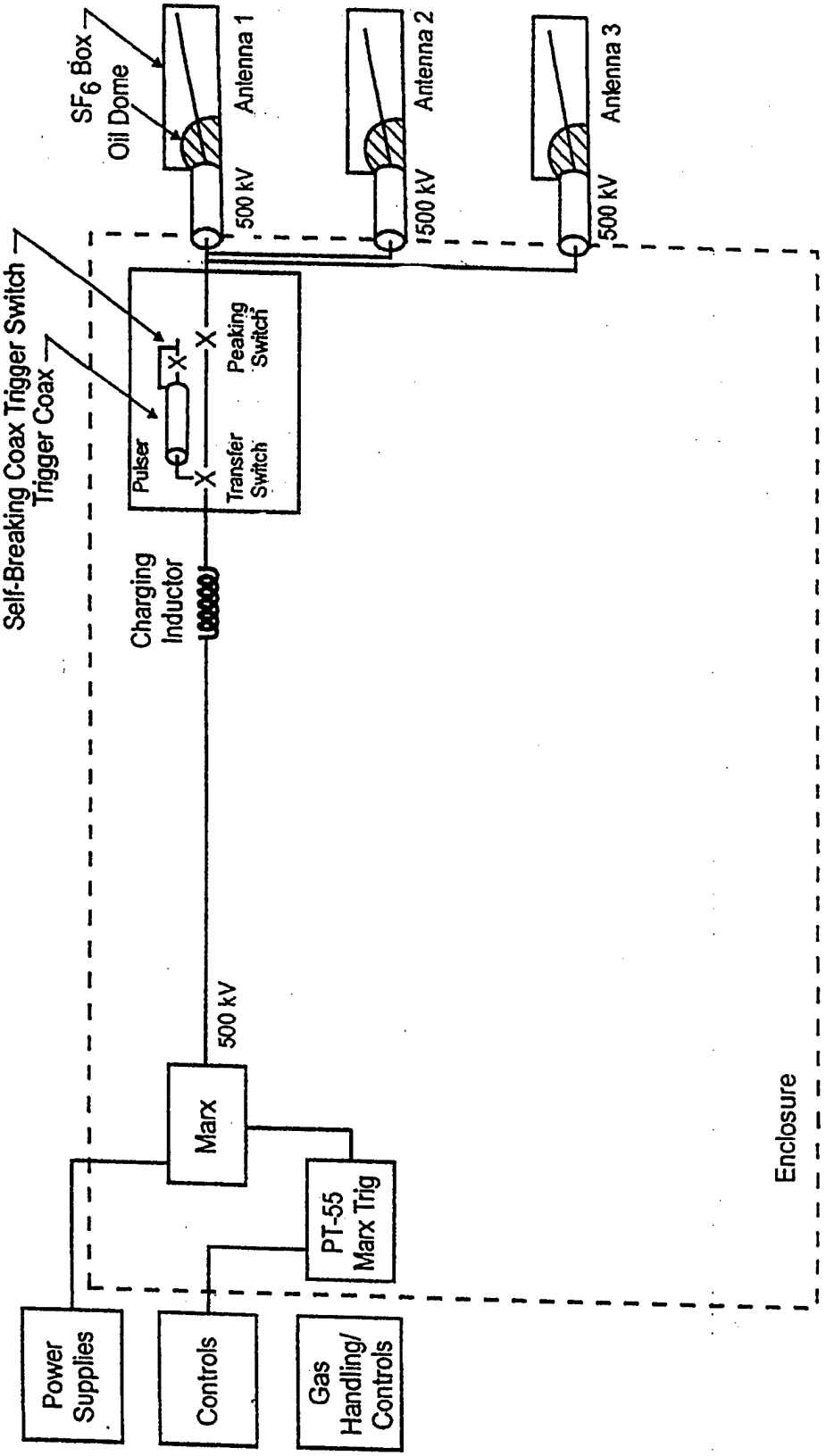

Figure 1. Block Schematic of the Testbed Pulser and the Radiating Sytem

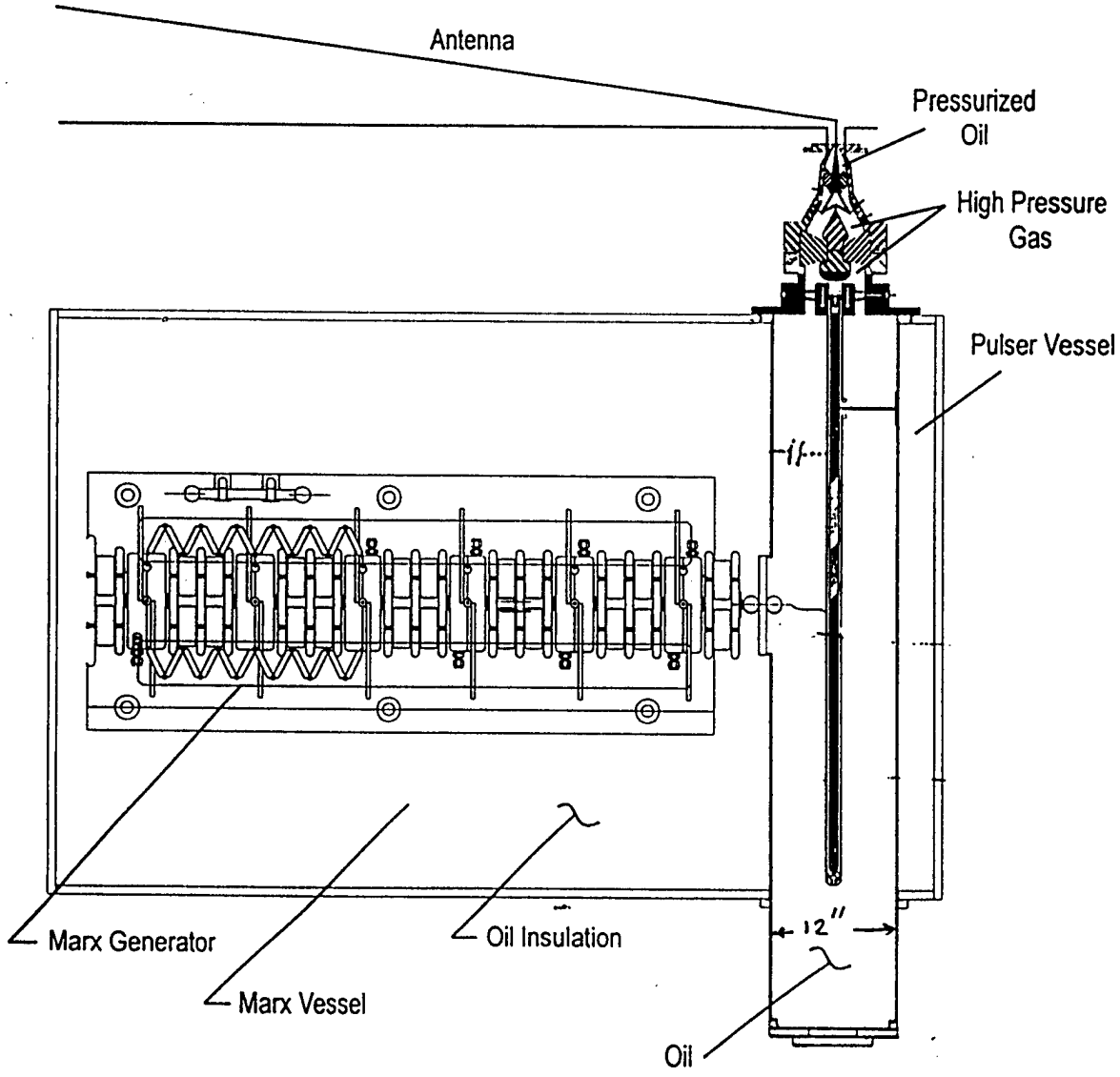

Figure 2. The Marx and the Testbed Pulser with a Vertical Axis

4. The Pulser as a Testbed System

4.1 Design Approach

The conceptual approach has utilized the most promising techniques for low jitter triggering and fast risetime output. At the same time, the design approach was made practical enough so that it would not require any major breakthroughs for it to make the transition from the laboratory to the field.

The design revolved around a circuit (see figure 3) that employed a 500 kV Marx generator (CM) that charged a transfer capacitor (CT) in a variable time between 20 to 200 ns depending on the value of the series charging inductance (LM) used. The triggered switch (S1) was to be the focus of the investigation in a subsequent program phase.

When the switch (S1) is triggered, a peaking capacitor (CP) is charged very rapidly in a time less than about 1.5 ns and switched out to the load through the self-breaking gas-insulated output switch. For practical antennas, the load is assumed to be between 67 and 135 ohms.

This circuit gives the most flexibility for varying the parameters of interest. The choice of the Marx generator was made to enable the charge times of the triggered switch to be varied between 20 ns and 200 ns. The charge time of the transfer capacitor and switch was to be varied by adjusting the series charging inductor between about 1.5 uH and 100 uH. Originally a thyratron based transformer circuit was intended to be used but it was quickly realized that the minimum charge times achievable with readily-available transformers were on the order of 150-200 ns. This long a charge time may turn out to be alright but previous triggering data indicate that charge times closer to 20 nsec produce much better triggering characteristics in terms of jitter and multi-channeling. Thus to explore the full range of charge times, the Marx was felt to be the best choice.

Although a transformer-based circuit could have achieved a higher rep-rate, the Marx would be able to achieve at least 50 Hz if desired and if the trigger circuit and

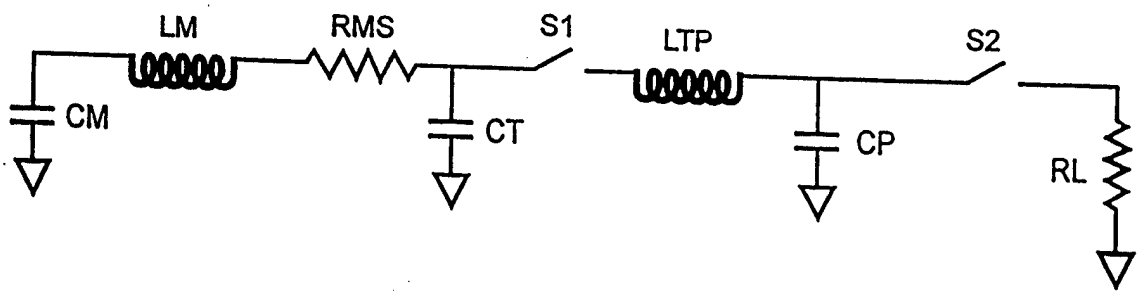

CM	Marx Capacitance	130 pF / 500 kV
LM	Marx Inductance	1.5 μH - 100 μH
RMS	Marx Series Resistance	2 ohms
CT	Transfer Capacitance	75 pF
S1	Triggered Gap	
LTP	Peaking Capacitor Charging Inductance	100 nH
CP	Peaking Capacitance	23 pF
S2	Peaking Switch	
RL	Load Resistance/Impedance	67 ohms

Figure 3. Simplified Circuit

power supplies could keep up with this rate which will still be in an interesting operating regime.

The Marx design was based on several 500 kV class Marxes that is well established as sources for fast EMP systems. These Marxes have had jitter in the range of 3-5 ns when using a very simple trigger source. With a more sophisticated source it is probably possible that this jitter could be further reduced to 2-3 ns. The jitter of the Marx, however, should not play a significant role in the triggering investigation because events related to the triggering of the transfer switch, would have been synchronized from the output pulse of the Marx generator.

The physical configuration of the hardware concept is shown in Figures 4 and 5. Figure 4 shows the overall configuration in plan view. The Marx is contained within a metal box where it is immersed in SF6 for insulation. The output of the Marx penetrates the cylindrically-shaped pulser vessel through a feed thru bushing. This cylinder contains oil which insulates the high-voltage components and which will be pressurized to equalize the pressures across the thin interfaces between the high-voltage pressure gas and water-filled regions of the pulser. Figure 5 shows a closer look at the components that are the heart of the testbed. These components include the transfer capacitor (CT), the triggered gas transfer switch (S1), the peaking capacitor(CP), peaking switch (S2), trigger transmission line, and the trigger source switch.

The transfer capacitor will be approximately 75 pF, but actually of somewhat smaller value, to account for other stray capacitance of the adjacent surfaces. Its dielectric has been chosen to be water because an interface was required to separate the high pressure gas from the surrounding oil insulation, and using the interface for a containment for the water was only a slight extension from a single interface. It also produces a more desirable lumped capacitive element as opposed to a distributed capacitor as would be the case if a lower permittivity dielectric were used. This feature will be particularly important if the triggered switch risetime proves to be low enough to drive the load directly and the stored energy in the capacitor must be taken out quickly.

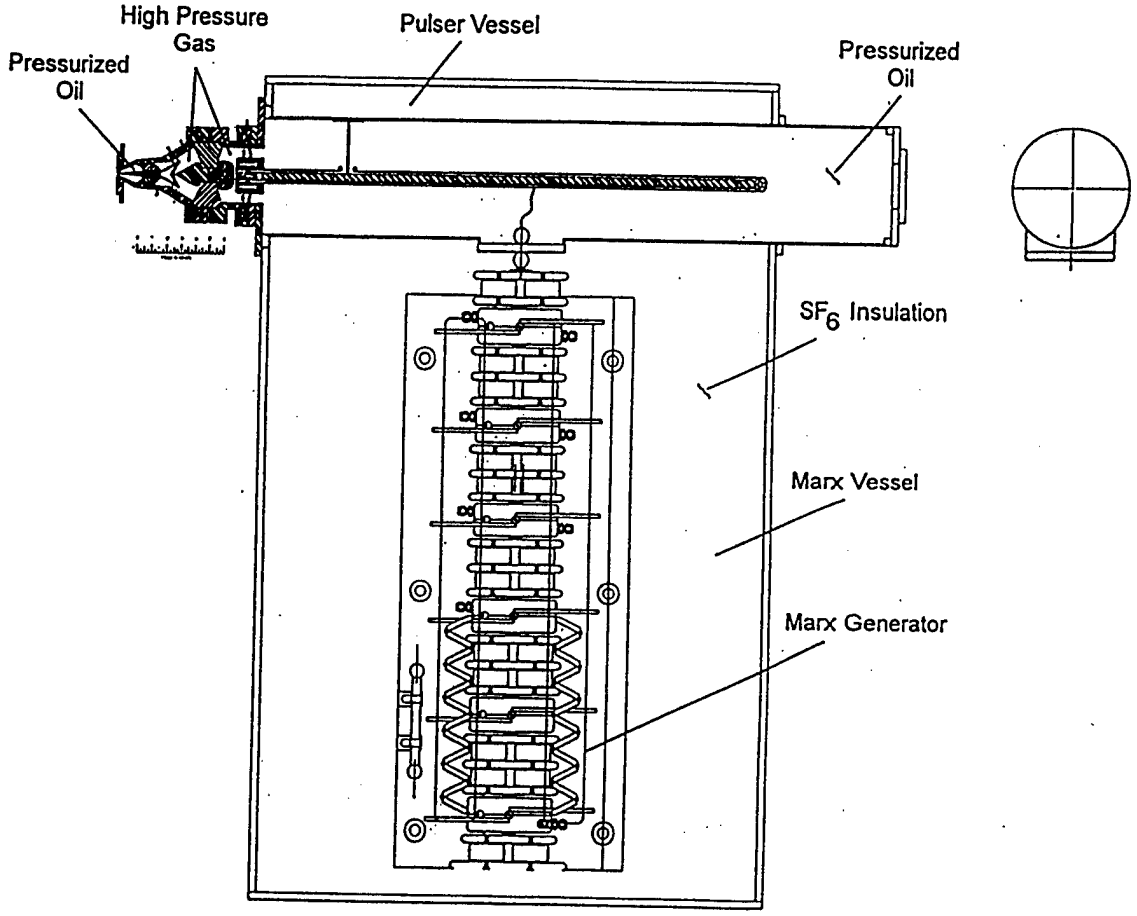

Figure 4. Overall Configuration : Plan View

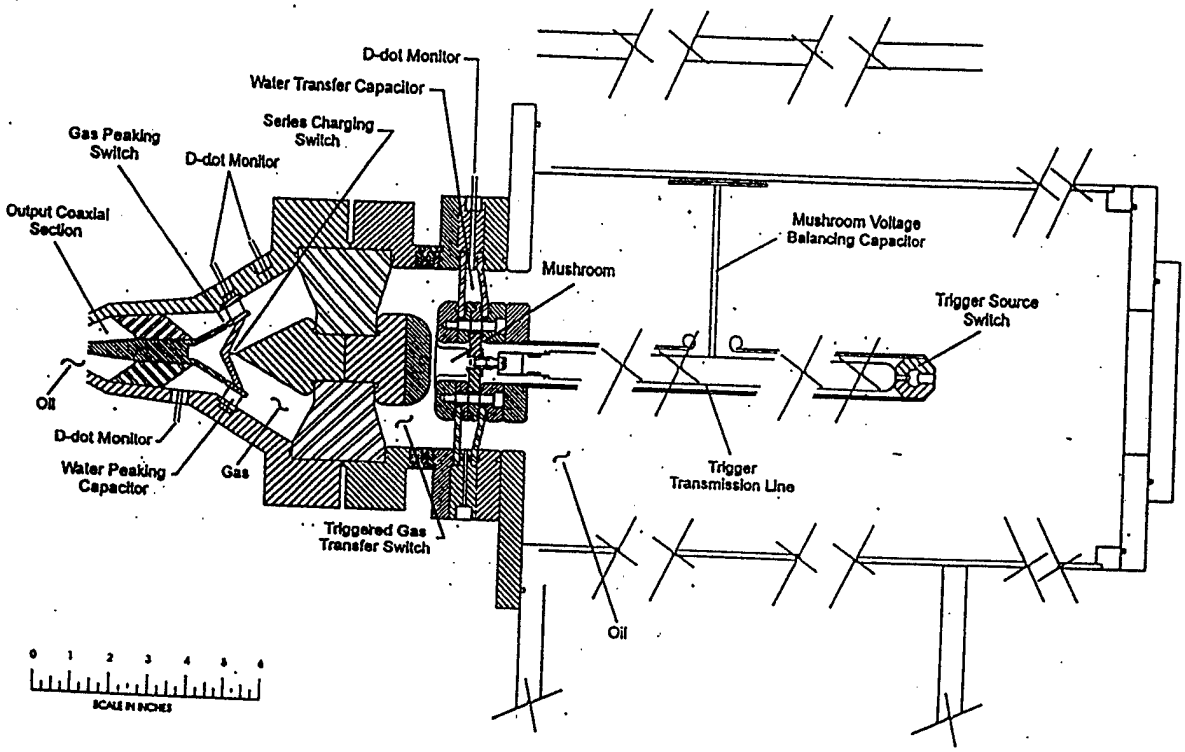

Figure 5. Switch Configuration

The transfer capacitor is sized to operate in the long 200 ns charge time mode at 500 kV at approximately 50% of JCM breakdown in negatively enhanced polarity.

The triggered switch region will be designed for a 100 atm. pressure of any gas and will be independent of the adjacent output switch region which will also be capable of a 100 atm. pressurization. Thus, each switch could use a different gas at a different pressure than the other.

The triggered switch employs a mushroom trigger electrode that will be optimally placed somewhere between 1/10 and 1/5 of the main gap spacing. The mushroom will be directly coupled to the 15-20 ohm trigger source transmission line. This transmission line will be adjustable in length from 12-24 inches and is connected at its other end to the self-breaking high pressure gas trigger source switch.

When the Marx charges the central coaxial region of the transfer capacitor and switch, the mushroom will follow the charge voltage at a potential that corresponds to its physical spacing within the switch gap region. For example, if the mushroom is placed at 20% of the gap spacing towards the charged electrode, at any time it would be at 80% of the voltage of the full gap with its final potential being 400 kV when the full switch voltage is 500 kV.

To force this voltage division, the dominant capacitive coupling across the trigger transmission line must also be capacitively coupled to ground. This is accomplished by bringing a lead out of the trigger transmission line and connecting it to a plate that can be placed in proximity to ground. For the mushroom placed at 1/5 the full gap spacing, the voltage across the trigger transmission line would be 100 kV when the switch full voltage is 500 kV.

At a predetermined time during the charging of the transfer capacitor and switch, the trigger source switch at the end of the trigger transmission line will self-break and launch an equal and opposite fast rising pulse down the transmission line, which will double at the mushroom end and swing the mushroom electrode voltage to increase the voltage across the large side of the gap sufficient to break the large gap of the triggered switch first. The trigger source switch's self-break voltage will be adjustable by means of pressure and gap adjustment.

This gap will be very similar to the gap used in the 100 kV IRA pulser and will also use H_2 at ~100 atm. to produce a very fast (~ few 100 ps) risetime. Based on experience, the timing of the trigger pulse arrival will be such that the main switch is triggered when it reaches about 80% of its self-break voltage.

This technique of triggering the mushroom switch with a close coupled transmission line and fast rising (estimated to be ~ 1 ns 10-90%) trigger pulse has been demonstrated by PSI. The results showed that approximately 10 or more spark channels were consistently produced using SF_6 at 14 atm. of pressure. It is this very fast risetime of the triggering pulse that will now be used that is expected to produce a very low jitter in the triggered switch in addition to many channels.

The peaking capacitor will be water-filled and will have a value of about 23 pF. We estimate the charge time of the capacitor to be about 1.5 ns. The capacitor is sized to operate at about 50% of JCM breakdown in negative charge polarity.

The peaking capacitor will be fabricated from a conical-shaped piece of plastic having conical-shaped annular endplates that encapsulate at least 12 cells containing the water dielectric.

The peaking capacitor is aligned in a specific way for two reasons. The first is the necessity to place the peaking switch in a position where it can be illuminated by the UV from the series charging switch and the second is to provide a good launch geometry to preserve the risetime of the switch onto the output coaxial section.

The series charging switch is placed in series with the charging of the peaking capacitor so that as the capacitor charges the arc that is created floods the peaking switch region with ultra violet. Four thin spokes hold this switch in place which allow virtually all of the UV to reach the peaking switch. Flooding a switching region while applying the voltage to breakdown levels in times shorter than the formative time of the switch (on the order of 1.5 ns) causes diffuse breakdown, i.e. bulk breakdown of the gas producing extremely fast risetimes on the order of 10's of ps as reported in the literature.

The coaxial output section of the source will be designed to be approximately 67 ohms and to preserve in risetime of the peaking switch while transitioning from gas to plastic and oil.

For laser triggering, the electrodes of the transfer switch will be replaced with a new set consisting of the charged electrode having a small diameter hole in it for the beam to go through and the other also having a small hole for the beam to dump into. A new sealed tube will replace the transmission line outer conductor which will be pressurized with gas along with the transfer switch. The far end of the tube will be sealed with a quartz window to allow the laser beam to enter. A focussing lens will be located just outside the quartz window.

We intend to use a YAG laser operating in the quadrupled 266 nm wavelength. We have had great success triggering 100 kV SF_6 gaps with 1 cm gap spacings with jitter of 130 ps using only about 10 mJ of laser light.

It has been found that about 10^{10} watts/cm^2 is required for laser triggering with SF_6 and using this YAG which has about 125 mJ of energy of 266 nm light will be more than sufficient to trigger the 500 kV switch.

4.2 Utility of the System

As mentioned previously, the primary focus of the program was to investigate low jitter switching and develop a conceptual layout of the design. The two candidates that would be tested in a subsequent Phase-II program are the electrical and laser triggering because of their known capabilities of producing low sub-nanosecond jitter switch-out. We intend to add another element to these methods by extending the parameter space to different gases, higher pressures, and in the case of electrical triggering to faster risetime and more closely-coupled trigger sources. What we expect to achieve with the electrical triggering is ultra-low jitter with fast risetime brought about by multi-channeling and low inductance. With the laser trigger, we expect to achieve low jitter.

The reason for setting the two simultaneous goals of low jitter and inductance is to ultimately make it possible to directly drive many cables from a single triggered switch configured in a launching geometry which would preserve the risetime of the switch itself. This way the number of triggered units could be minimized and the many cable outputs of each could be adjusted in lengths to achieve steering capability for an array.

If we had only a low jitter switch, its inherent inductance would limit the risetime into a low impedance multi-cable array thus requiring the secondary output switching stage.

A significant part of Phase-II effort would be to choose possible gas and gas mix candidates and fully characterize them in terms of breakdown voltage versus pressure, effective stress time of the applied voltage and polarity effects on breakdown. In addition, we would look at the recovery characteristics for limited rep-rates, assuming the trigger and charging circuits are capable of rep-rate. Once these characteristics are established, their triggerability would be evaluated. Typical gases that would be tested include, but was not limited to air, N_2, SF_6, H_2 , Argon and their mixtures.

To accomplish the task of characterizing the gases, the test bed will have the trigger mushroom and trigger transmission line removed and electrodes of known enhancement and gap spacing installed. Sets of near-uniform field electrodes would be used as well as sets with a moderate and a highly enhanced electrode on one side. In this way the polarity of the Marx could be reversed and the polarity effect on breakdown observed.

At the same time the risetime characteristics of the gases can be studied as a function of field, pressure, etc., and with and without UV illumination by observing the peaking switch output waveform. The peaking switch would be more useful than the triggered transfer switch for obtaining this data because the output coaxial section geometry would preserve much of the switch's risetime unlike the transfer switch which will be geometrically risetime-limited by nature of its size and shape.

Table 2 gives the typical ranges of effective stress times for the two switches.

Table 2. Effective Stress Times for the two Switches

Operating Mode	Transfer Switch (S1)	Peaking Switch (S2)
t(eff) = 200 ns charge time (slow charge)	25 ns	300 ps
t(eff) = 20 ns charge time (fast charge)	3 ns	300 ps

Breakdown data from the literature for N2, H2, SF6, and an SF6/air mixture are plotted with the stress times at which the data was taken in Figure 6. Based on these numbers, we can expect the peaking switch which has an effective risetime of !0.3 nsec to achieve perhaps 8-9 MV/cm at 100 atm. with N2 or about 3 MV/cm at 100 atm. with H2. With a nominal enhancement of perhaps 1.6, the typical gap spacing range will be about 0.1 – 0.26 cm for the peaking switch.

For the triggered transfer switch, scaling by $t_{eff}^{-1/6}$ to the longer stress times, (assuming the same scaling as air and SF6 at moderate pressures), we anticipate a spacing range of 0.15 to 0.38 cm for the fastest charging and about 0.21 to 0.55 cm for the slowest at 100 atm. while operating at 80% of self-break. In reality, the pressure may have to be reduced to enable more practical spacings for which a reasonable mechanical tolerance can be maintained.

Table 3 shows the fields that could be achieved in the two switches with N2 and H2 gas at 100 atm.

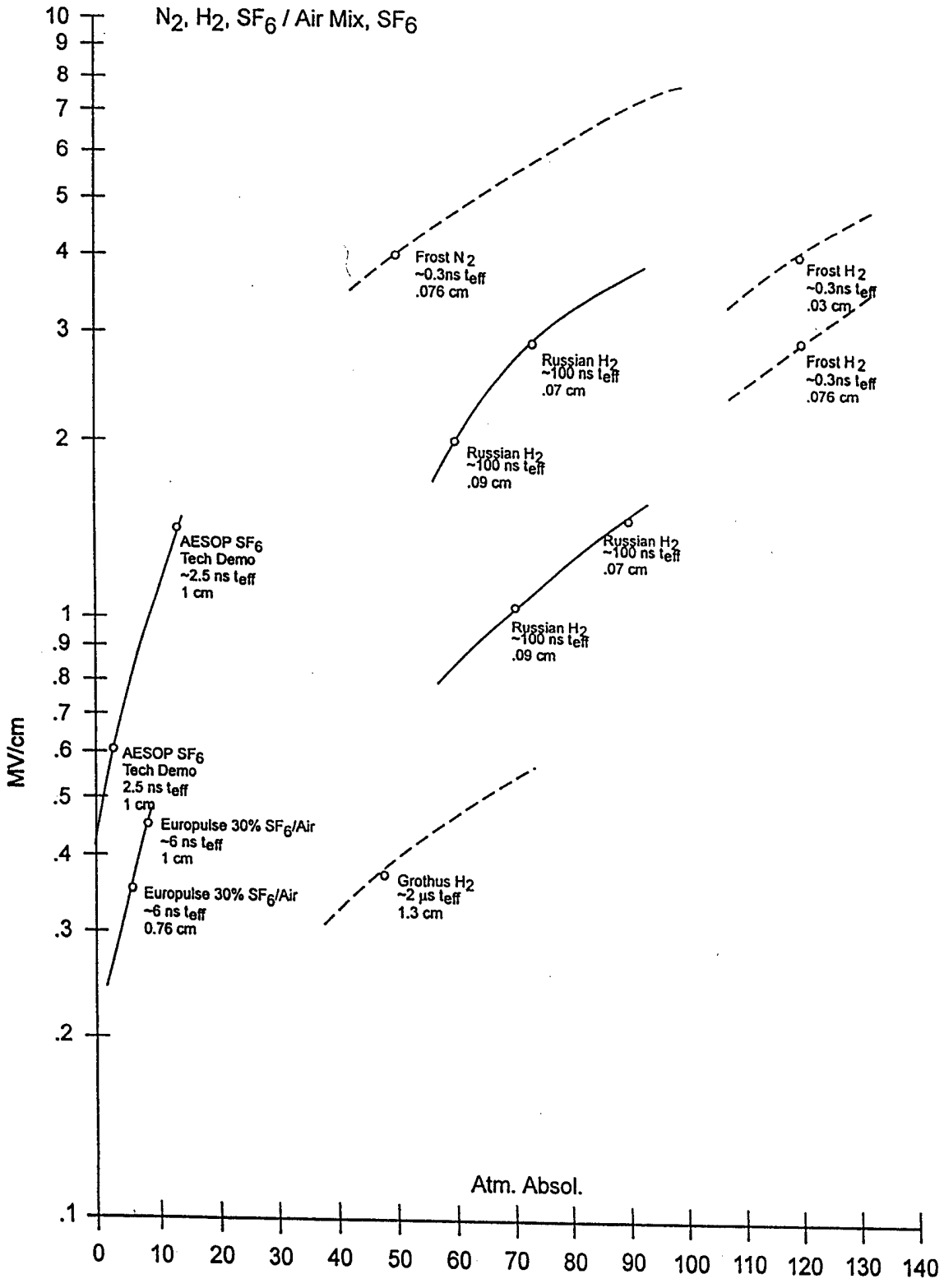

Figure 6. Gas Breakdown Data

TABLE 3. Fields that could be achieved with Nitrogen and Hydrogen gas at 100 atm.

Transfer Switch	N_2	H_2
Slow charge	3.8 MV/cm	1.4 MV/cm
Fast charge	5.4 MV/cm	2.0 MV/cm
Peaking switch	8 MV/cm	3 MV/cm

Using the resistive phase formula

$$T_R = \frac{158\sqrt{\rho/\rho_o}}{Z^{1/3}\,E^{4/3}}\ ns \quad 10-90\%$$

where ρ_o = STP density of air

ρ = density of gas at operating pressure

Z = driven impedance

E = field in units of 10 kV/cm

and the inductive risetime given by

$$T_L = 2.2\,\frac{L}{Z} \quad 10-90\%$$

and taking the quadrature addition of the two to estimate the total risetime, we expect the total risetimes at 100 atm. of pressure for the two switches which are listed in Table 4.

TABLE 4. Expected Risetimes for the two Switches at 100 atm.

	N_2			H_2		
	T_R	T_L	T_{total}	T_R	T_L	T_{total}
Transfer switch single channel	142 ps	137 ps	197 ps	144 ps	360 ps	387 ps
slow charge	92 ps	98 ps	134 ps	91 ps	250 ps	266 ps
fast charge						
Transfer switch multi-channel (6 channels)						
slow charge	78 ps	22 ps	81 ps	79 ps	60 ps	99 ps
fast charge	50 ps	16 ps	52 ps	50 ps	42 ps	65 ps
Peaking switch	*	7 ps	*	*	17 ps	*

*a similar VU illuminated switch was reported to have risetime of 10's of picoseconds implying very small resistive phase risetime of < 10's of picoseconds.

From the above table it is clear that with multi-channeling, the possibility of obtaining a very fast risetime in the 100 ps regime while driving perhaps 67-Ohm cables without a peaking circuit is real.

4.3 Measurements

Jitter and risetime measurements will be made using fast risetime D-dot monitors strategically placed throughout the pulser. The D-dots will be made from 0.125-inch diameter copper jacketed coaxial cable cut square and inserted through the outside of the coax surface or water capacitor ground conductor until flush with the inside surface. This type of construction has been proven to have risetimes of 10's of picoseconds. These monitors will be calibrated and by numerical integration one can observe the voltage waveform anywhere the monitors are placed.

The D-dot signal itself will be used as a time mark for purposes of measuring the jitter of the two gas switches. The t' time mark will be when the self-breaking trigger source switch closes, and the jitter of the triggered switch will be determined from the time this pulse traverses

the transmission line and the output voltage from the triggered switch is detected. Likewise, the jitter of the peaking switch will be determined from the arrival time of the output from the triggered switch and the time of detection of the output of the peaking switch.

A slight difficulty arises in measuring the t' time because the trigger transmission line is at high voltage. In this case, we have two choices. The first is to use a high speed photo detector (~150 ps risetime) which will detect the light flash of the trigger source switch through a fiber optic link. Another possibility is to transit time isolate a hard-coupled cable to the trigger transmission line, which is a common technique. In the case of the laser trigger, we will use a fast photo-detector to detect the incoming laser beam to provide the initial time mark. In summary, based on data from the literature as well as risetime calculations, we expect risetimes out of the peaking circuit approaching 10's of ps.

5. Description of the Radiating System

5.1 Canonical Input Waveforms to the Radiating System

Let us consider a canonical pulsed waveforms as follows:

(a) half-cycle at 1 GHz

In designing any antenna system, it is imperative to know the Fourier spectrum of the input signal fed to the antenna. This is essential in optimally designing the antenna system so that it can efficiently radiate the significant frequency components of the input signal without introducing dispersion.

The required spectra are analytically derived and the magnitudes of the spectra are also plotted. We use the following definition of the Fourier integral pair.

$$f(t) = \frac{1}{2\pi} \int_{-\infty}^{\infty} \tilde{F}(\omega)\, e^{j\omega t}\, d\omega \quad ; \quad \tilde{F}(\omega) = \int_{-\infty}^{\infty} f(t)\, e^{-j\omega t}\, dt \qquad (1)$$

5.2 Half-Cycle Sine Wave

This pulsed-voltage waveform is a half-cycle sine wave at 1 GHz, denoted by $f_v(t)$, and is given by

$$f_v(t) = \begin{cases} V_0 \sin(\omega_0 t) & \text{for } 0 \le t \le T/2 \\ 0 & \text{for all other times} \end{cases} \qquad (2)$$

with

$\omega_o = 2\pi f_o$; $f_o = 1$ GHz $\equiv$ fundamental frequency

$T \equiv$ "period" $= (1/f_o) = 1$ nsec .

Its Fourier spectrum is given by:

$$\tilde{F}_V(\omega) = \int_0^{T/2} V_0 \sin(\omega_0 t)\, e^{-j\omega t}\, dt \ . \qquad (3)$$

Using the identity

$$\int e^{ax} \sin(bx)\, dx = \frac{e^{ax}}{\left(a^2 + b^2\right)} \left[a \sin(bx) - b \cos(bx)\right] . \qquad (4)$$

We find the spectral magnitude of the half-cycle sine wave to be

$$\left|\tilde{F}_v(\omega)\right| = \left| \frac{2 V_o\, \omega_o \cos(\omega T/4)}{\left(\omega_o{}^2 - \omega^2\right)} \right| \qquad (V/Hz) \ . \qquad (5)$$

The half-cycle sine wave $f_v(t)$ and its magnitude spectrum $\left|\tilde{F}_V(\omega)\right|$ are shown plotted in Figure 7. This pulse has a peak voltage of 1 volt and the dc component of its spectrum is given by setting $\omega = 0$ in (5) as $\tilde{F}_V(o) = 2V_o/\omega_o = 3.18 \times 10^{-10}$ (V/Hz) for the assumed values of $V_o = 1$ V and $f_o = 1$ GHz or $T = 1$ nsec. This dc value is also seen in the spectral magnitude plot of Figure 7. What is evident here is that the half - cycle sine wave is an extremely wideband pulse with frequency components extending from dc to several GHz, depending on what we consider as significant spectral content at higher frequencies. The first null in the spectrum occurs at the third harmonic or $f = 3$ GHz, corresponding to $\omega T/4 = 3\pi/2$ or $f = 3 f_o$. Subsequent nulls are at $\omega T/4 =$

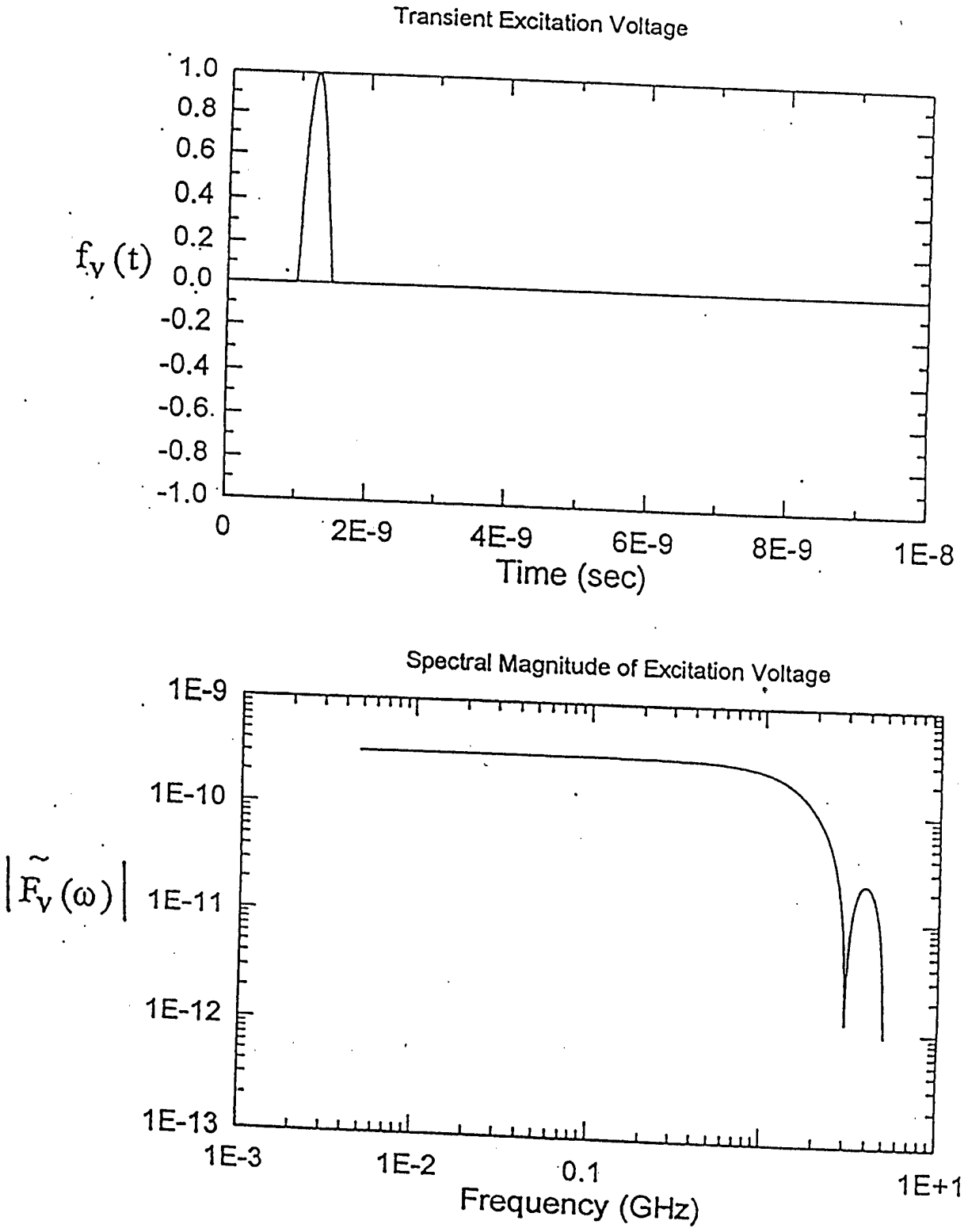

Figure 7. The Half-cycle Sine Wave and its Spectral Magnitude

$5\pi/2$, $7\pi/2$ etc. of f = 5 GHz, 7 GHz, .. etc. The conventional 3 dB bandwidth of this spectrum extends from dc to about 1.19 GHz.

6. Prediction of Far Fields for a Single Antenna Element

We have chosen a TEM horn as an example of the antenna array element. A TEM horn, schematically shown in Figure , is basically an individual spherical TEM element in the array. This type of a radiating element has been analyzed in the past [5,6,7,8] and its performance characteristics, especially on bore-sight are known in closed form. For example, with reference to Figure 8,

2a ≡ maximum width of the TEM horn along the magnetic field direction

2b ≡ maximum separation between the plates of TEM horn along the electric field direction

z = 0 ≡ aperture plane

V(t) ≡ driving voltage of each element.

One of the first questions we need to address is the TEM impedance or the characteristic impedance of the spherical TEM mode propagating in the TEM horn. This is purely resistive. We can now examine, if there is an optimal TEM impedance. While the plates are 2a wide and separated by 2b in the aperture plane, they are 2a' wide and 2b' apart at the "source plane". It is not essential, but mechanically convenient to impose the condition (b'/a') = (b/a), resulting in flat plates of triangular shapes. We can now consider the impedances seen by the sources. As the individual sources are turned on, it takes some finite time for each element to be impacted by the presence of other elements. Consequently, at early times (or high frequencies), the impedance seen by the source is simply the characteristic impedance of the TEM mode in an infinitely long conical line which may be written as

$$Z_{early} = Z_o \, f_g \left(b'/a'\right) \qquad (6)$$

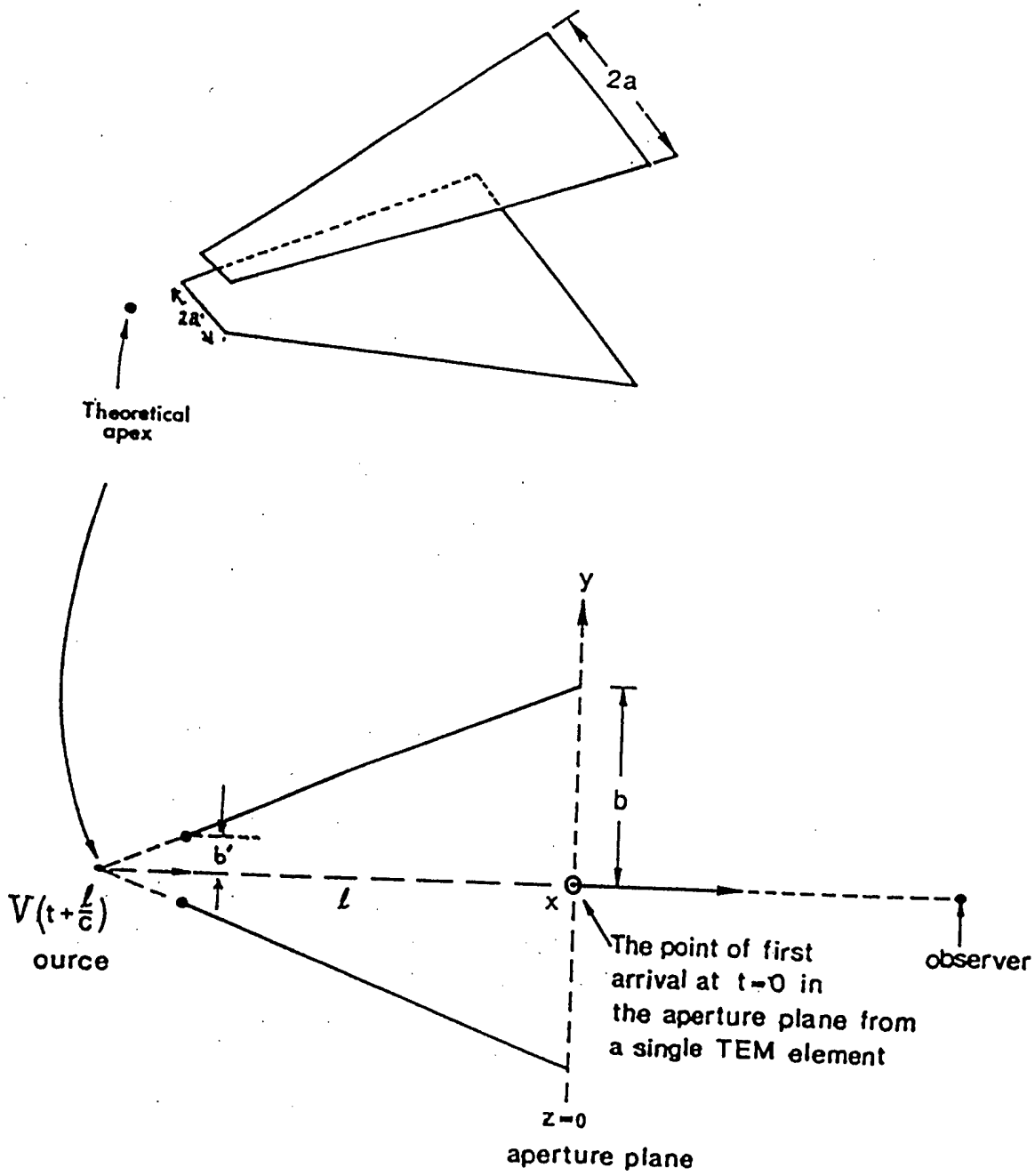

Figure 8. A spherical TEM horn element and its source point in the aperture plane

$Z_o = \sqrt{\mu_o/\varepsilon_o}$ = characteristic impedance of free space and f_g is a tabulated geometric factor, which is a function of the parameter (b'/a'). As time progresses, the mutual interactions between elements will occur, resulting in late times, in the launching of spherical TEM waves in both plus and minus z-directions. The very late-time impedance can then be written as

$$Z_{late} = \frac{1}{2} Z_o (b/a) \tag{7}$$

The factor of (1/2) accounts for waves in both forward and backward directions. If we now desire or require that the early and late time impedances be equal, this gives

$$\frac{1}{2}\frac{b}{a} = f_g (b'/a') = f_g (a/b) \tag{8}$$

For this special case, we get (b/a) = (b'/a') = 0.877 and $Z_{early} \cong Z_{late} \cong 165$ ohms. For example, a convenient choice would be

$$\begin{array}{llllll} 2b = 21 \text{ cm} & , & b = 10.5 \text{ cm} \\ 2a = 28 \text{ cm} & , & a = 14 \text{ cm} \\ \lambda = 20 \text{ cm} & , & (b/a) = 0.75 \end{array} \tag{9}$$

$$(\lambda/b) = 1.905 \quad \rightarrow \quad Z_c^{(TEM)} \cong 150 \text{ ohms} .$$

Next we turn our attention to computing the radiation from the individual antenna element (TEM horn above). This has been accomplished using the commercially available NEC-2 code on an IBM-PC desk-top computer. Because of the symmetry, it is adequate to consider the upper half of the antenna, which has been modelled successively by 1,3,5 and 7 wires in the NEC-2 code. The method of moments equations are adequate to evaluate all the individual wire segment currents (j = 1 to N, where N is the total

number of segments). Once the segment current distributions are evaluated, the electromagnetic fields are then determined by an integration of these currents with appropriate Green's functions. The modelling guideline of NEC-2 requires that the longest segment be no longer than tenth of the shortest wavelength of interest. This guideline is strictly followed. Once the current distribution on all wire segments are known, the radiated fields calculation is straightforward and performed efficiently by NEC-2. Initially we assume a delta function (in time) voltage source and get the radiated field (impulse response) at 512 (= 2^9) frequency points. This impulse response is then multiplied by the Fourier spectrum of the pulsed waveforms of interest and plotted in frequency domain. The frequency domain radiated fields are then Fourier inverted using an FFT (fast Fourier transfer) routine that gives time-domain plots at $2x512 = 2^{10} = 1024$ points.

The radiated fields in the form of $\left| \; r\tilde{E}_\theta(\omega) \; \right|$ and ($r\, E_\theta\, (t)$) are plotted in the horizontal plane ($\theta = 90^\circ$) for varying ($\phi = 90^\circ$, 60°, 30° and 0°) and in the vertical plane ($\phi = 0^\circ$) for varying ($\theta = 90^\circ$, 60°, 30° and 0°). These plots are shown in Figure 9 for the half-cycle sine wave pulse input. Such computations can be performed, once the precise waveshapes out of the testbed pulser are known from analysis or measurement.

7. Optimization of a Three Element Array

Under Phase-II, we are proposing to study an array of three TEM horns , energized from a single source, wherein known amounts of excitation time-delays can be introduced. Consider a three element array as shown in figure 10. Each of the antenna elements in figure 10 is an UWB transmitter (e.g., TEM horn). We are proposing to analytically and experimentally investigate the performance of a set of three TEM horns. The purpose here is to maximize or combine the signals from individual elements, along a prescribed direction, denoted by the observer location P(x,y,z) in figure 10.

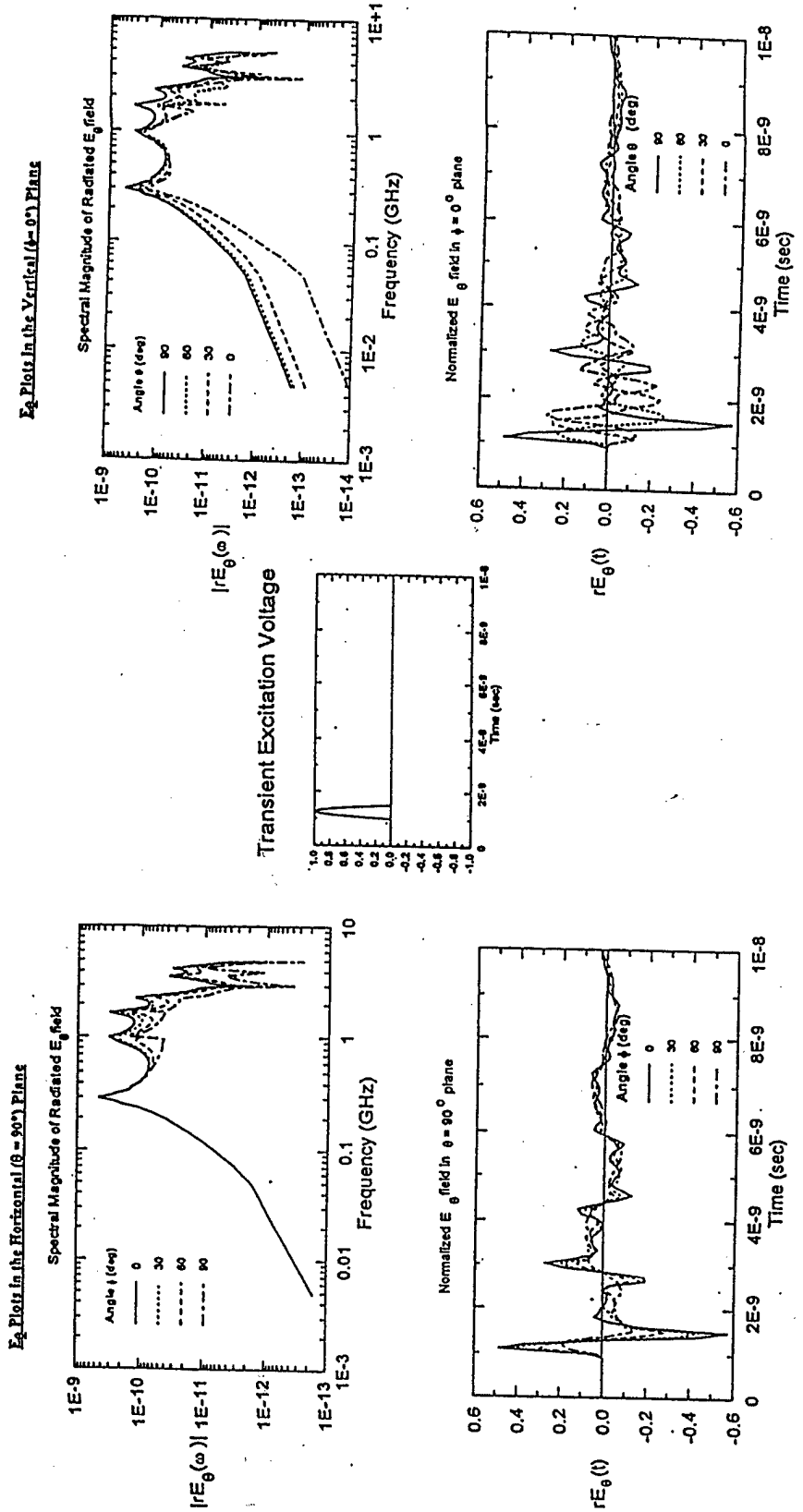

Figure 9. Radiated Electric Field from an Individual TEM horn in the two planes for the case of a Half-cycle Sine Wave Input Shown in the Middle

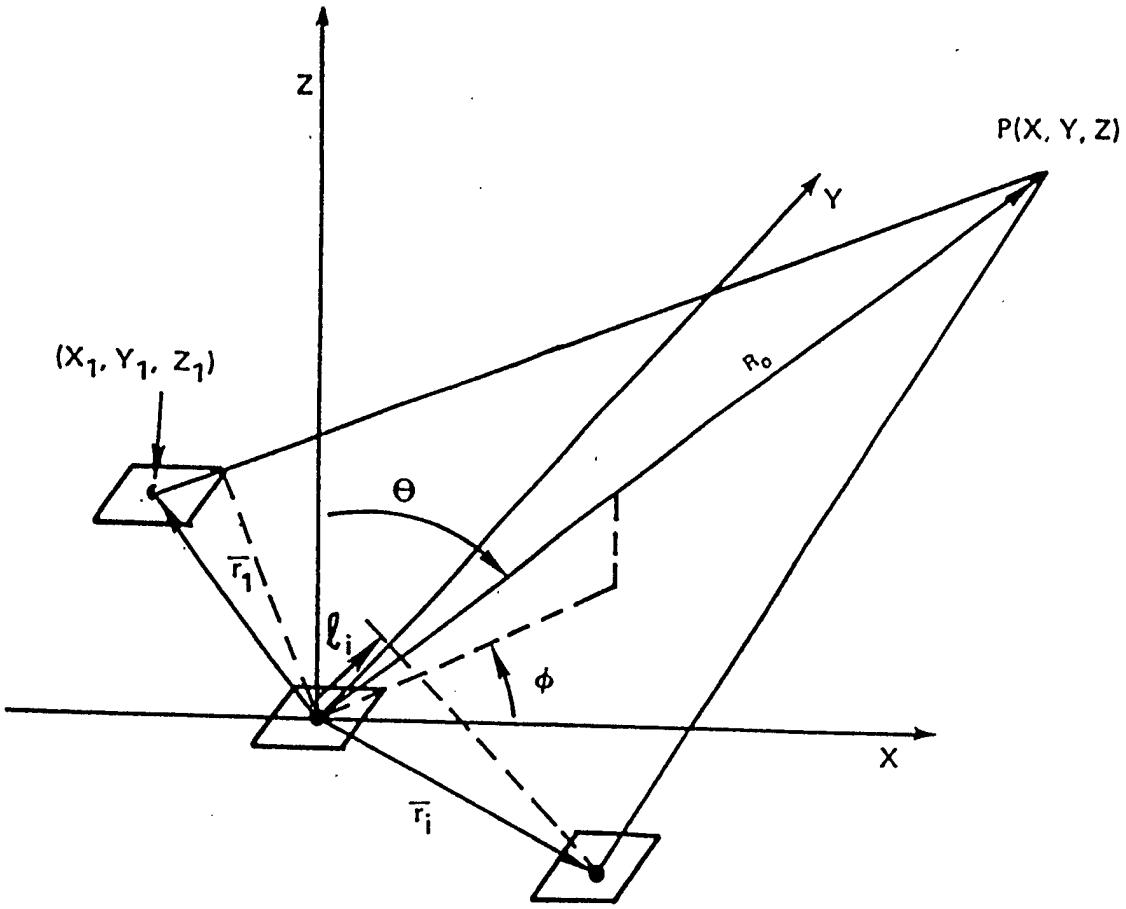

Figure 10. A Generalized Timed-Array Antenna Distribution

We do know the radiated far-electric field from TEM horns (earlier section) and the requirement is to adjust the timing (or the triggering sequence) of each of these elements so that the UWB beam is radiated along a prescribed direction.

A distinction needs to be made between the classical phased-array antennas and these timed-array antennas. Phase is a frequency domain concept and time-delay is its equivalent in the time-domain. Phased -array antennas are typically narrow-band, while we are dealing with extremely broad-band signals here. In phased-array antennas, the individual elements do not interact thus leading to the use of array factor. The radiation pattern of the array is then the

radiation pattern of a single element times the array factor. In the present, timed-array antennas, the individual elements **can be** in electrical contact with its neighboring elements, in the aperture plane. This has the benefit of enhancing the low-frequency performance of the array. So, unless the individual TEM horns are distinct and separate from each other, the concept of array factor does not apply.

After the timing sequences are known , we can numerically introduce known amounts of jitter (excitation time delays) to evaluate the jitter requirements.

8. Objectives of Phase–II Effort :

8.1 Introduction to Phase-II

Phase-II is anticipated to take 19 months from the start of the program to completion. Four major subtasks comprise the schedule for the technical work which are the design, modeling, fabrication and assembly, and testing. These are shown in the schedule in figure 11 along with the two remaining non-technical subtasks of management and shipping.

In the first month of the program, we would expect to meet with the technical contract monitor to review the technical goals of the program and fine- tune the conceptual design of the system to best achieve these goals.

Following the affirmation of the conceptual design, we anticipate approximately 3 months of preliminary design followed by 2 months of final design. Completion of the design is scheduled to occur at 6 ½ months after program start and would constitute the first milestone of the program. A preliminary design review is scheduled to occur at the completion of the preliminary design followed by the final design review which is scheduled to coincide with the 6 ½ month milestone date.

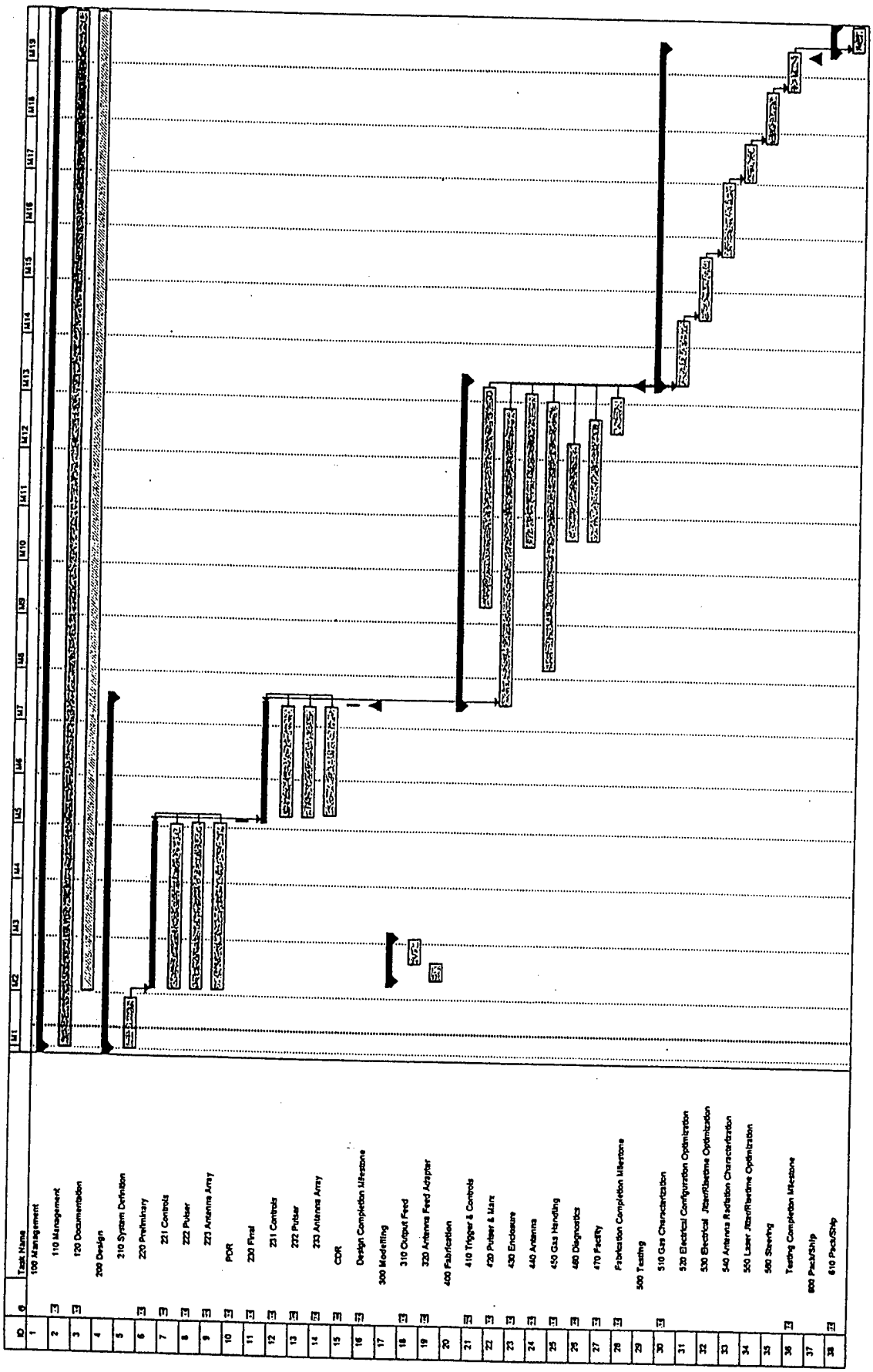

Figure 11. Milestone and Schedule for the Proposed Phase-II Effort

During the design task and early enough for the results to be incorporated into the design, we will perform some physical modeling of two critical regions. These regions are critical to generating and preserving a risetime in the range of 50psec. and would be virtually impossible to accurately model analytically.

The fabrication and assembly subtask follows the design milestone and is scheduled to have a duration of 6 months. At 12 ½ months into the program we would expect the system to be ready for checkout. This point in time would constitute the second milestone of the program.

The testing and technically the most important task in the program is scheduled to take 6 months. During this period of time all candidate gases for use in the system will be fully characterized and both electrical and laser triggering techniques will be evaluated. The triggered switch performance will be optimized to produce the least jitter to enable synchronization of to another event. The culmination of the program will be the application of synchronized switching to steer a beam produced by an array of 3 antennas.

The completion of this synchronization demonstration will constitute the third milestone of the program which is expected to occur at 18 ½ months after program start.

Finally, during the last 2 weeks of the program, the hardware will be packed and shipped to its ultimate destination as designated by the funding agency unless otherwise required in a Phase-III program.

8.2 Phase-II Technical Objectives

The objective of Phase-II will be to demonstrate the ultra-low jitter of a triggered, fast risetime gas switched pulser and apply the most promising technique of triggering it to synchronizing 3 pulsers to steer the beam from a 3 antenna linear array. The goal of this demonstration will be to show the concept's commercial potential in any of the following four

applications which will require precise timing of the electromagnetic output of a pulser to another event.

In effect, any of the four applications would use a common building block which would be a precisely timed, modular pulser unit that when ganged together and driving a large array of antennas, the full potential of ultra-low jitter switching would be realized. A precisely timed array would enable one to produce a higher field at a longer distance and to steer it.

The four areas of application requiring precisely timed UWB sources that have been identified as the most commercially feasible are as follows:

- Directed energy weapon for electronic warfare
- Above and below ground transient radar for target location and discrimination both for military related objects and commercial objects such as pipes, etc.
- Interference testing equipment of military equipment
- Space debris detection radar

In addition, if the triggering techniques produce multi-channeling within the switch as expected, the resulting low inductance would produce a fast enough risetime to drive multiple cables directly, thus avoiding the use of a second stage of pulse sharpening. This would immensely simplify the construction of the array by reducing the complexity of the pulser and reducing the number of pulsers required for driving the array.

The specific technical performance goals of pulser are summarized in Table 5.

TABLE 5. Technical Performance Goals

Output Voltage	~500 KV
Output Risetime (10-90%)	~100 psec.
dV/dt	$\geq 5 \times 10^{15}$ V/sec
Pulse Length(e-fold)	~5nsec
Rep-Rate	
electrical triggered	50 Hz
laser triggered	~10 Hz
Driven Impedance	~67-135 ohms
Jitter goal(1σ rms)	10-20 psec

The techniques that will be employed in triggering the gas switch to achieve ultra-low jitter will be an extension of techniques previously used for very low jitter. For example, we

have laser triggered a dc charged 100 KV switch in the our laboratory and achieved 130 psec. (1σ rms) jitter. There is no reason to believe that this was the limit because there was no effort made to explore the full range of gas types, pressures charge times, etc. because there was no necessity to achieve a lower jitter.

In another example, we achieved electrical triggered multi-channeling which produced an extremely consistent number of channels around a 4 inch diameter trigger electrode at 1 MV. Such consistency implied an extremely low jitter. We intend to extend this technique by using a faster rising trigger pulse in the range of $\leq$ 200 psec risetime achieved by carefully matching the trigger pulse transmission line to the trigger electrode and using a high pressure hydrogen switch to initiate the trigger pulse.

Because we are starting with proven methods for producing low jitter and fast risetime and drawing from research data in the literature, although extending them to the new regimes, we have a high level of confidence that we will succeed in achieving the stated goals.

8.3 Deliverable Hardware under Phase-II

The following hardware and services will be provided as part of the Phase-II program.

- The complete design for the described pulser system with the appropriate drawings
- The complete operable pulser test bed system hardware including:
  - A single pulser for use in the gas characterization experiments and the steering demonstration
  - Two additional pulsers and additional hardware to enable the 3 pulsers to be used in the steering experiment
  - Three antennae and other hardware to enable radiating and steering a beam
  - A control subsystem including a console, power supplies, gas handling and gases
  - Components to enable electrical triggering and laser triggering
- Facility space at PSI San Leandro to perform the experiments
- Use of the presently available YAG laser
- Documentation including

- Monthly status reports
- Final scientific and technical report summarizing the results of the gas characterization, jitter measurements, risetime measurements, radiated waveform measurements, and steering demonstration
- Operation and Maintenance manual

References:

[1] F.J.Agee, W.D.Prather, J.M.Lehr, W.Scholgield and J.Gaudet, " Ultra-Wideband Source Research: Gas,Oil and Solid Sate Switching, 1998.

[2] J.J.Mankowski, "High-Voltage Subnanosecond Dielectric Breakdown"' Ph.D. Disseratation, Texas Tech University, December 1997.

[3] J.M.Lehr, C.E.Baum and W.D.Prather, " Fundamental Physical Considerations for Ultrafast Spark Gap Switching," Switching Notes, Note 28, 1 June 1997.

[4]. S. Mercer, I. Smith and T. Martin, " A Compact Multi-Channel Gas Switch," Proc. International Conference on Energy Storage and Switching, Asti, 1974.

[5] I.Smith and V.Carboni, " The Use of Triggered Multichannel Gas Spark Gaps to Produce Nanosecond Risetimes, " , HDL Contract DAAL02-86-C-0073 and AFWL F29601-87-C-0201, presented at the Advanced Pulse Power Conference, BDM International, 1990

[6] W.Frey, "Low-Intensity Laser-Trigeering of Rail-Gaps with Magnesium-Aerosol Switching Gasses," Forschungszentrum Karlruhe, Herman-von Helmholtz-Platz, D76344 Eggenstein/Leopoldshafen.

DISTRIBUTION LIST

AUL/LSE
Bldg 1405 - 600 Chennault Circle
Maxwell AFB, AL 36112-6424 1 cy

DTIC/OCP
8725 John J. Kingman Rd, Suite 0944
Ft Belvoir, VA 22060-6218 2 cys

AFSAA/SAI
1580 Air Force Pentagon
Washington, DC 20330-1580 1 cy

AFRL/PSTL
Kirtland AFB, NM 87117-5776 2 cys

AFRL/PSTP
Kirtland AFB, NM 87117-5776 1 cy

Pro-Tech 1 cy
1630 North Main Street, #377
Walnut Creek, CA 94596-4609

Official Record Copy
AFRL/DEHP/Dr Jane Lehr
3550 Aberdeen Avenue SE
Kirtland AFB, NM 87117-5776 5 cy